Molecular Structure of Tetracarbonyldihydroiron: Microwave Measurements and Density Functional Theory Calculations

Brian J. Drouin and Stephen G. Kukolich*

Contribution from the Department of Chemistry, The University of Arizona, Tucson, Arizona 85721

Received December 8, 1997

Abstract: Microwave spectra of seven isotopomers of tetracarbonyldihydroiron were measured in the 4−16 GHz range using a Flygare−Balle type microwave spectrometer. Measured transitions were fit using a rigid rotor Hamiltonian with five independent distortion constants. Structural parameters from a least-squares fit to the rotational constants are r(Fe−H) = 1.576(64) Å, r(Fe−C1) = 1.815(54) Å, r(Fe−C3) = 1.818(65) Å, r(C1−O1) = 1.123(80) Å, r(C3−O3) = 1.141(74) Å, ∠(H−Fe−H) = 88.0(2.8)°, ∠(C1−Fe−C2) = 154.2-(4.2)°, ∠(C3−Fe−C4) = 99.4(4.3)°, ∠(Fe−C1−O1) = 172.5(5.6)°, and ∠(Fe−C3−O3) = 177.8(6.8)°. All of the carbonyl groups are bent slightly *toward* the hydrogen atoms. The least-squares-determined structural parameters are in excellent agreement with the substitution coordinates determined from the Kraitchman equations, the structural parameters calculated using density functional theory, and the previously published electron diffraction data. The C_{2v} molecular symmetry is consistent with the results of the microwave data and with theoretical calculations. All of the analyses show that the H atoms are separated by about 2.2 Å, and this indicates that the complex is clearly a "classical dihydride" rather than an η^2-"dihydrogen" complex. Structural parameters obtained from a density functional theory calculation agreed with measured values to within 2%. The density functional theory analysis of the anharmonicity in the Fe−H symmetric stretching potential is shown to support the observed deuterium isotope effects observed for the hydrogen atom coordinates. The anharmonicity effects are larger for the Fe−H stretching coordinate than for the ∠H−Fe−H interbond angle. The r_0(Fe−D) bond lengths were observed to be 0.05(4) Å shorter than the r_0(Fe−H) bond lengths.

Introduction

There has been a high level of interest in transition metal hydrides over the past 20 years because they are involved in a wide variety of reactions which are useful in chemistry and the chemical industry. They are important intermediates in catalytic processes such as hydroformulation and hydrogenation.[1−4] They have also been useful as stoichiometric reagents in organic and organometallic syntheses.[5] The reactions of transition metal hydrides show a variety of patterns of reactivity,[6] with examples of hydride donors,[6] protonating agents,[7] and hydrogen atom transfer.[8] Microwave spectra have been obtained previously for the mononuclear hydrides $HCo(CO)_4$,[9] $HMn(CO)_5$,[10] and $HRe(CO)_5$.[11]

More recently, much attention has been focused on transition metal complexes containing two H atoms. The unexpected discovery by Kubas et al.[12] in 1984 of dihydrogen complexes, in which the H−H bond remains intact with the H−H bond length very close to that of a free hydrogen molecule, initiated a large number of searches for other complexes of this type. The hydrogen atom separation for dihydrogen complexes is typically $r_{HH} \cong 0.8$ Å, very close to the free hydrogen molecule value of $r_{HH} = 0.74$ Å. Dihydrogen complexes are believed to be of fundamental importance in a wide variety of processes,[13] ranging from hydrogenation of alkenes or alkynes to understanding the functioning of metalloenzymes such as hydrogenases[14] or nitrogenase.[15] The rapid progress in this area and many of the large number of dihydrogen complexes discovered recently are discussed in an extensive review by Jessop and Morris.[16] Theoretical developments regarding various dihydrogen complexes are reviewed in the book by Dediu.[3] Hydrogen atom coordinates are often poorly determined using X-ray diffraction, and the X-ray structure alone is not usually considered to give a reliable identification of dihydrogen complexes. Microwave spectroscopy can provide highly accurate hydrogen atom positions through isotopic substitution analysis. Previous microwave work on $H_2Os(CO)_4$[17] showed that this complex is a classical dihydride.

Even though the $H_2Fe(CO)_4$ complex is quite reactive, it was previously studied using gas-phase electron diffraction,[18] but

(1) Hlatky, G. G.; Crabtree, R. H. *Coord. Chem. Rev.* **1985**, *65*, 1.
(2) Crabtree, R. H. *The Organometallic Chemistry of the Transition Metals*; John Wiley & Sons: New York, 1988; Chapter 34.
(3) Dediu, A. *Transition Metal Hydrides*; VCH Publishers: New York, 1992; Chapter 5.
(4) *Transition Metal Hydrides*; Muetterties, E. L.,Ed.; Marcel Dekker: New York, 1971.
(5) Eisenberg, D. C.; Lawrie, C. J. C.; Moody, A. E.; Norton, J. R. *J. Am. Chem. Soc.* **1991,** *113*, 4888.
(6) Martin, B. D.; Warner, K. E.; Norton, J. R. *J. Am. Chem. Soc.* **1986,** *108*, 33.
(7) Longato, B.; Martin, B. D.; Norton, J. R.; Anderson, O. P. *Inorg. Chem.* **1985,** *24*, 1389.
(8) Edidin, R. T.; Norton, J. R. *J. Am. Chem. Soc.* **1986**, *108*, 948. Wegman, R. W.; Brown, T. L. *J. Am. Chem. Soc.* **1980**, *102*, 2494.
(9) Kukolich, S. G.; Sickafoose, S. M. *J. Chem. Phys.* **1996,** *105,* 3466.
(10) Kukolich, S. G.; Sickafoose, S. M. *Inorg. Chem.* **1994,** *33*, 1217.
(11) Kukolich, S. G.; Sickafoose, S. M. *J. Chem. Phys.* **1993,** *99*, 6465.
(12) Kubas, G. J.; Ryan, R. R.; Swanson, B. I.; Vergamini, P. J.; Wasserman, H. J. *J. Am. Chem. Soc.* **1984**, *106*, 451. Kubas, G. J. *Acc. Chem. Res.* **1988,** *4*, 120.
(13) Henderson, R. A. *Transition Met. Chem. (London)* **1988,** *13*, 474.
(14) Adams, M. W. W.; Mortenson, L. E.; Chen, J.-S. *Biochim. Biophys. Acta* **1981,** *594*, 105.
(15) Orme-Johnson, W. H. *Annu. Rev. Biophys. Chem.* **1985,** *14*, 419.
(16) Jessop, P. G.; Morris, R. H. *Coord. Chem. Rev.* **1992,** *121*, 155.
(17) Kukolich, S. G.; Sickafoose, S. M.; Breckenridge, S. M. *J. Am. Chem. Soc.* **1996,** *118*, 205.

S0002-7863(97)04158-9 CCC: $15.00
Published on Web 06/23/1998

no information on internal motion was obtained. Evidence for internal motion was obtained by Vancea and Graham[19] from ^{13}C NMR measurements in which a single resonance indicates fluxional behavior that renders the two types of C atoms equivalent on the NMR time scale. Vancea and Graham[19] suggest an intermolecular CO exchange process to explain the behavior. However, internal motion would be very likely if this were a "dihydrogen" complex, and internal rotation of the dihydrogen group could couple with motion of the CO groups to render them equivalent through an intramolecular process.

Experimental Section

Samples of the compound, tetracarbonyldihydroiron, were synthesized using the following reaction scheme outlined by Vancea and Graham.[19]

$$KOH + Ba(OH)_2 + Fe(CO)_5 \xrightarrow[12\ h]{H_2O} K^+_{(aq)} + Ba^{2+}_{(aq)} + Fe(CO)_4^{2-}{}_{(aq)} + CO_{(g)} + OH^-_{(aq)} \quad (1)$$

$$Fe(CO)_4^{2-}{}_{(aq)} + H_2SO_{4(l)} \xrightarrow[0\ °C]{H_2O} SO_4^{2-}{}_{(aq)} + FeH_2(CO)_{4(g)} \quad (2)$$

This method was dubbed the "polar night synthesis" because reaction 2 was done outdoors at −20 °C, at night. The "polar night" was not available in the Sonoran desert, so both steps of the reaction were performed in a darkened laboratory, and the crucial second step (reaction 2) was performed in an ice bath at 0.4 °C. Although no direct measurements of the yield were made, it is likely that the higher temperature for reaction produced a lower hydride yield. The product was collected during the course of reaction 2 by condensation in a trap surrounded by liquid nitrogen. The sample is light and heat sensitive, decomposing in about a 0.5 h under fluorescent light at room temperature. It is extremely air sensitive and must be handled under vacuum or inert atmosphere at all times. The observed decomposition products are colored deep red.

A gas-phase infrared spectrum was obtained for characterization of the product. For the observed spectra, $Fe(CO)_5$ was found to be a significant impurity. In these samples, the characteristic yellow (when frozen) color of the iron pentacarbonyl was easily visible in contrast to the white color of the dihydride. The two compounds could be separated by fractionation through a − 40 °C ethanol/H_2O slush bath into a −196 °C $N_{2(l)}$ trap. The $Fe(CO)_5$ remained in the warmer trap, while the more volatile hydride passed into the $N_{2(l)}$ trap. At 1 cm^{-1} resolution, the purified compound shows six transitions in the carbonyl stretching region. Four transitions were not fully resolved, but major peaks were near 2014 and 2052 cm^{-1}. The measured frequencies are 2015 (s), 2014 (s), 2035.0 (m), 2052 (s), 2053 (s), and 2077.6 (w) cm^{-1}. The intensities of the strong lines varied greatly with pressure, which was difficult to control due to the high volatility and temperature sensitivity of the compound.

Deuterated samples were prepared by using D_2O in both steps of the reaction and D_2SO_4 in step 2. Very little deuterium substitution was observed when only D_2SO_4 was used in normal (H_2O) solvent. This may be an indication of either (single) protonation prior to step 2, to produce the hydridic anion instead of the dianion, or rapid exchange of the dihydride with the acidic solvent immediately following step 2. Even though the reaction was carried out in D_2O, the presence of many proton sources (the hydroxide groups and trapped water in the $Ba(OH)_2$ lattice) in the reactions resulted in all three of the isotopomers, $D_2Fe(CO)_4$, $HDFe(CO)_4$, and $H_2Fe(CO)_4$, in the product mixture. From the relative intensities of the measured microwave transitions, it would appear that the HD and H_2 products were in approximately equal concentration, each of which being about 3 times the concentration of the doubly deuterated isotopomer.

(18) McNeill, E. A., Scholer, F. R. *J. Am. Chem. Soc.* **1977**, *99*, 6243.
(19) Vancea, L.; Graham, W. A. G. *J. Organomet. Chem.* **1977,** *134*, 219.
(20) Bumgarner, R. E.; Kukolich, S. G. *J. Chem. Phys*. **1987,** *86,* 1083.

Table 1. Measured and Calculated Transition Frequencies (MHz) for $^{56}FeH_2(CO)_4$

measured[a]	calculated	difference	J	K_p	K_o	J'	K_p'	K_o'
4463.0245(08)	4463.0237	0.0008	1	0	1	2	1	1
5010.1381(10)	5010.1375	0.0006	1	1	0	2	2	0
5064.4045(18)	5064.4068	−0.0023	2	2	0	3	1	2
5096.0327(08)	5096.0325	0.0002	1	1	1	2	2	1
5240.5653(05)	5240.5647	0.0006	2	1	1	3	0	3
6863.7593(23)	6863.7580	0.0013	3	1	2	4	0	4
6952.8798(10)	6952.8792	0.0006	2	1	1	3	2	1
7099.1849(12)	7099.1859	−0.0010	3	2	1	4	1	3
7169.2765(10)	7169.2761	0.0004	2	1	2	3	2	2
7740.3730(03)	7740.3727	0.0003	2	2	0	3	3	0
7760.9950(09)	7760.9960	−0.0010	2	2	1	3	3	1
7767.5525(26)	7767.5526	−0.0001	4	2	3	5	1	5
8811.4986(17)	8811.5005	−0.0019	3	0	3	4	1	3
8941.5080(19)	8941.5078	0.0002	3	1	2	4	2	2
9292.2394(29)	9292.2347	0.0047	33	3	3	4	2	3
9639.7880(39)	9639.7881	−0.0001	5	3	3	6	2	5
9673.5165(19)	9673.5163	0.0002	3	2	1	4	3	1
9763.8721(10)	9763.8705	0.0016	3	2	2	4	3	2
10455.8041(23)	10455.8056	−0.0015	3	3	0	4	4	0
10458.7839(19)	10458.7842	−0.0003	3	3	1	4	4	1
10999.7972(28)	10999.7956	0.0016	4	1	3	5	2	3
11101.9908(26)	11101.9912	−0.0004	4	0	4	5	1	4
11461.8085(39)	11461.8085	0.0000	4	1	4	5	2	4
11580.6743(25)	11580.6741	0.0002	4	2	2	5	3	2
11799.5412(21)	11799.5401	0.0011	4	2	3	5	3	3
12416.1537(29)	12416.1545	−0.0008	4	3	1	5	4	1
12435.6159(21)	12435.6170	−0.0011	4	3	2	5	4	2
13141.9475(14)	13141.9474	0.0001	5	1	4	6	2	4
13163.4912(28)	13163.4928	−0.0016	4	4	0	5	5	0
13163.8390(38)	13163.8425	−0.0035	4	4	1	5	5	1
13438.1607(24)	13438.1599	0.0008	5	0	5	6	1	5
13495.4015(51)	13495.4042	−0.0027	5	2	3	6	3	3
13671.7747(22)	13671.7757	−0.0010	5	1	5	6	2	5
13876.2091(38)	13876.2078	0.0013	5	2	4	6	3	4
15869.9179(59)	15869.9145	0.0034	5	5	1	6	6	1

[a] Numbers in parentheses following measured transition frequencies represent the standard deviation in the last digits before the parentheses.

Microwave Measurements

Microwave spectra were measured in the 4−16 GHz range using a Flygare−Balle type spectrometer system.[20] Transition frequencies are typically measured with 1−6 kHz accuracy, depending on the intensity of the transition and the presence of nearby unresolved lines. Systematic errors are believed to be much less than 1 kHz since the local frequency standard is quite stable and is regularly calibrated using WWVH (Boulder, CO). This complex is unstable above −40 °C, but, fortunately, it is quite volatile, even down to −60 °C. A small glass sample chamber is attached to a series 9 General Valve pulsed nozzle, and this whole assembly is maintained at −50 °C. The sample is transferred into the glass chamber under vacuum, and approximately 1 atm of neon gas is introduced after the transfer is complete. The neon carrier gas is periodically resupplied as the chamber pressure drops due to opening the pulse valve. The sample temperature is controlled by the presence of an ethanol/water/dry ice slush bath that completely surrounds the glass cell and pulsed valve. The bath temperature is adjusted to produce a sample vapor pressure of a few Torr. Strong signals were observed for the main isotopomer, with a signal-to-noise ratio of ∼200/1. The signal decreased only upon cooling the sample below −55 °C and disappeared quickly below −60 °C. For expedient data collection on the less abundant iron and ^{13}C isotopomers, it was necessary to keep the temperature near −50 °C, a temperature that provided good signal without rapid loss of sample due to high volatility or decomposition. Transitions due to the ^{56}Fe (89.7%) isotopomer gave the strongest signals; these were shadowed on either side by the ^{54}Fe (5.7%) and ^{57}Fe (2.2%) isotope lines. The two sets of ^{13}C lines were also measured in natural abundance (2.0%). The lines for both deuterated isotopomers had good signal-to-noise ratio and were readily measured using the sample synthesized with D_2SO_4 in D_2O. Thirty-five lines were measured for the main isotopomer and are listed in Table 1, along with assignments and calculated best-fit frequencies, and these include several $\Delta K_o = 2$ transitions. The inclusion of the

Table 2. Measured Transition Frequencies (MHz) for $^{54}FeH_2(CO)_4$ and $^{57}FeH_2(CO)_4$

$^{54}FeH_2(CO)_4$[a]	dev[b]	$^{57}FeH_2(CO)_4$[a]	dev[b]	J	K_p	K_o	J'	K_p'	K_o'
4464.8235(06)	−0.0001	4462.1367(17)	0.0000	1	0	1	2	1	1
5012.2219(21)	−0.0018	5009.1122(11)	0.0001	1	1	0	2	2	0
5098.3745(08)	−0.0012	5094.8801(17)	0.0002	1	1	1	2	2	1
6955.4309(11)	−0.0015	6951.6228(15)	0.0000	2	1	1	3	2	1
7172.3841(24)	0.0013			2	1	2	3	2	2
7743.7871(29)	0.0003			2	2	0	3	3	0
7764.5240(11)	−0.0003	7759.2593(10)	−0.0002	2	2	1	3	3	1
9677.1708(26)	0.0013			3	2	1	4	3	1
10460.5711(23)	0.0011			3	3	0	4	4	0
10463.5732(13)	0.0007	10456.4241(18)	0.0001	3	3	1	4	4	1
13169.9221(27)	−0.0011			4	4	1	5	5	1

[a] Numbers in parentheses following measured transition frequencies represent the standard deviation in the last digits before the parentheses. [b] The deviation between measured and calculated values.

Table 3. Measured Transition Frequencies (MHz) for $^{56}FeHD(CO)_4$ and $^{56}FeD_2(CO)_4$

$^{56}FeHD(CO)_4$[a]	dev[b]	$^{56}FeD_2(CO)_4$[a]	dev[b]	J	K_p	K_o	J'	K_p'	K_o'
4439.0964(07)	0.0024			1	0	1	2	1	1
4972.4219(14)	−0.0002	4935.5091(15)	0.0016	1	1	0	2	2	0
5056.4997(06)	−0.0003	5017.6562(14)	0.0009	1	1	1	2	2	1
6564.9635(05)	−0.0001			2	0	2	3	1	2
6910.0140(16)	−0.0010	6867.8326(01)	0.0016	2	1	1	3	2	1
7121.6794(08)	−0.0002	7074.5915(37)[c]	0.0018	2	1	2	3	2	2
7678.3998(06)	−0.0005	7617.7733(24)	−0.0019	2	2	0	3	3	0
7698.6729(16)	−0.0004	7637.6090(20)	−0.0019	2	2	1	3	3	1
8767.4261(05)	−0.0014	8722.5312(56)	−0.0003	3	0	3	4	1	3
8892.7489(25)	−0.0013	8844.3384(18)	−0.0003	3	1	2	4	2	2
9235.5513(16)	0.0008			3	1	3	4	2	3
9606.2743(24)	0.0019	9540.4968(25)	0.0010	3	2	1	4	3	1
9695.0210(18)	0.0008	9627.3059(56)	0.0002	3	2	2	4	3	2
10369.9989(30)	−0.0010	10286.0345(30)	0.0007	3	3	0	4	4	0
10372.9411(10)	0.0009			3	3	1	4	4	1
10943.8339(42)	0.0013			4	1	3	5	2	3
11395.0509(38)	0.0002			4	1	4	5	2	4
11508.8575(24)	−0.0009			4	2	2	5	3	2
11723.5672(09)	−0.0005			4	2	3	5	3	3

[a] Numbers in parentheses following measured transition frequencies represent the standard deviation in the last digits before the parentheses. [b] The deviation between measured and calculated values. [c] This frequency represents the center of a doublet, presumably split by deuterium quadrupole coupling. The splitting is 29 kHz.

Table 4. Measured Transition Frequencies (MHz) for the ^{13}C-Substituted Isotopomers

$^{13}C1(ax)$[a]	dev[b]	$^{13}C3(eq)$[a]	dev[b]	J	K_p	K_o	J'	K_p'	K_o'
4438.6539(43)	0.0002	4448.6498(21)	0.0001	1	0	1	2	1	1
4998.2115(22)	−0.0010	4979.0742(37)	−0.0007	1	1	0	2	2	0
5083.0207(40)	−0.0012	5065.4728(09)	0.0006	1	1	1	2	2	1
6926.2720(19)	0.0000	6919.3395(37)	0.0000	2	1	1	3	2	1
7725.1662(10)	0.0008	7689.3623(12)	0.0003	2	2	0	3	3	0
7744.8072(33)	0.0013	7710.9045(12)	−0.0003	2	2	1	3	3	1
		8907.8070(38)	−0.0001	3	1	2	4	2	2
		9616.9819(47)	0.0003	3	2	1	4	3	1
10436.5543(10)	−0.0001			3	3	0	4	4	0
10439.2913(20)	−0.0005	10389.0331(56)	−0.0001	3	3	1	4	4	1

[a] Numbers in parentheses following measured transition frequencies represent the standard deviation in the last digits before the parentheses. [b] The deviation between measured and calculated values.

weaker $\Delta K_o = 2$ transitions allowed more accurate determination of the distortion constants. Tables 2−4 list measured and calculated rotational frequencies for the ^{54}Fe (11 lines), ^{57}Fe (6 lines), HD (19 lines), D_2 (11 lines), $^{13}C1_{ax}$ (8 lines), and $^{13}C3_{eq}$ (9 lines) isotopomers, respectively. The "ax" (axial) and "eq" (equatorial) subscripts correspond to carbon atoms 1,2 and 3,4 respectively, as shown in Figure 1. Several unidentified transitions were also measured that persisted after the sample chamber was warmed to room temperature. At least one of the decomposition products was quite volatile, as indicated by the ability to clean a sample cell with red deposits by simply evacuating it. Most of the unidentified lines were transient, indicating that they may be due to impurities with a different vapor pressure than that of $H_2Fe(CO)_4$ or to an intermediate compound only present during the initial decomposition process. The frequencies of these unidentified lines are 6339.7271(9), 6875.5098(31), 6875.5546(10), 6875.5837(5), 6875.6384(32), 7734.5390(16), and 7757.3090(4) MHz. The quadruplet at 6875 MHz appeared only while scanning the deuterated sample, indicating that this unknown compound may contain H (D) and the structure observed could be due to quadrupole coupling of the deuterium nucleus.

Data Analysis

The measured rotational transition frequencies were fit to the rotational constants A, B, and C and five distortion constants D_J, D_{JK}, D_K, δ_J, and δ_K. All of the measured lines, with the exception of the "impurity lines" discussed above, were assigned to allowed "c" dipole asymmetric top transitions. Extensive searches were carried out initially and in looking for weaker ^{13}C transitions, so it is very unlikely that allowed "b" or "a"

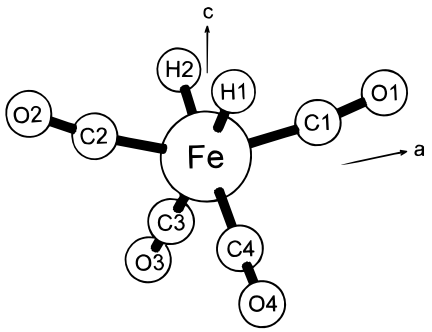

Figure 1. Molecular structure and atom numbering system for tetracarbonyldihydroiron. The axial carbonyl groups, C1−O1 and C2−O2, are at an angle of approximately 13° to the "*a*" principal axis.

Table 5. Best-Fit Spectral Parameters for $^{56}FeH_2(CO)_4$, $^{54}FeH_2(CO)_4$, and $^{57}FeH_2(CO)_4$[a]

parameter	units	$^{56}FeH_2(CO)_4$	$^{54}FeH_2(CO)_4$	$^{57}FeH_2(CO)_4$
A	MHz	1353.1369(4)	1353.7909(6)	1352.8158(2)
B	MHz	1036.6331(3)	1037.0151(7)	1036.4445(2)
C	MHz	926.7420(4)	926.7247(15)	926.7511(5)
D_J	kHz	0.153(9)	fixed	fixed
D_{JK}	kHz	0.38(3)	0.41(2)	0.41(2)
D_K	kHz	−0.24(3)	fixed	fixed
δ_J	Hz	−8(5)	fixed	fixed
δ_K	kHz	0.93(4)	fixed	fixed
σ_{fit}	kHz	1.8	1.4	0.3

[a] The listed uncertainties are 2σ.

dipole transitions exist for this complex. The spectrometer is not currently equipped with Stark plates, and thus no direct measurement of μ_c could be made. All seven parameters (listed in Table 5) were well determined by fitting the 35 lines for the normal isotopomer, $^{56}FeH_2(CO)_4$. The accurate determination of all the distortion constants was aided by the inclusion of several $\Delta K_o = 2$ transitions, which have greater dependence on these small parameters. All fits for the other six isotopomers (listed in Tables 5 and 6) include at least one fixed distortion parameter. Correlations between these values and the use of relatively small data sets would have made independent determination of all of the distortion constants difficult. When necessary, values of the distortion constants were fixed at those for the normal isotopomer since isotopic substitution is not expected to change distortion constants very much. Parameters that were varied are in excellent agreement with those determined using data for the normal isotopomer. All seven of the spectral parameter fits had standard deviations less than 2 kHz, and this is very close to the experimental uncertainties in the line positions.

The presence of *only* one set of lines for each of the single H(D) and C(^{13}C) substitutions verifies the C_{2v} symmetry of the molecule, i.e., the two H atoms are equivalent and carbons 1,2 and 3,4 are each equivalent, respectively. If the molecule did not possess C_{2v} symmetry, one or more of these substitutions would have produced two sets of lines corresponding to two possible nonequivalent positions for isotopic substitution. The observation of only "*c*" dipole transitions indicates perpendicular planes of symmetry, which is consistent with the C_{2v} symmetry assignment.

The symmetry of the molecule requires that the Fe atom lie directly on the "*c*" principal axis of the molecule. This location should make the *C* rotational constant invariant to Fe isotopic substitution. However, small deviations in the *C* values were obtained for different Fe isotopes, indicating that vibrational averaging effects, similar to those causing nonzero inertial defects for "planar" molecules, were contributing to the *C* rotational constants. *C* values for the ^{54}Fe and ^{57}Fe isotopomers show deviations of −17.3(1.4) and +9.1(6) kHz from the *C* value of the normal isotopomer.

The Molecular Structure

The structure of this complex was determined by carrying out a global, least-squares fit to the measured rotational constants to obtain the r_0 structural parameters and, in addition, doing a Kraitchman analysis to determine r_s parameters for many of the structural parameters. The large number of available rotational constants (21) allowed variation of all (assuming C_{2v} symmetry) of the independent structural parameters. Although no oxygen atom isotopic substitution data were obtained, the r(C−O) distances and ∠(Fe−C−O) parameters could be varied without problems in the fitting routine. Slightly better standard deviations for the fits could be obtained by fixing the r(C−O) distances and ∠(Fe−C−O) angles, but the variable parameters were in very good agreement for the 10-parameter and 6-parameter fits. For the 10-parameter fits, very reasonable values were obtained for C−O bond lengths and Fe−C−O angles. Deviations of the ∠(Fe−C−O) bond angles from linearity were only significant ($<2\sigma$) for the ∠(Fe−C1−O1) axial carbonyl angle. Both 8- and 10-parameter fits were performed in which the ∠(Fe−C−O) angles were fixed at 180° and then allowed to vary for comparison. The standard deviations of the two fits are similar, and the resulting parameters were nearly equal, indicating that the fit did not improve much by the addition of the extra parameters. However, since there are correlations between parameters, we believe the most accurate (but not necessarily the most precise) structural parameters are obtained using the 10-parameter fit. Except for the ∠(Fe−C−O) angles, all parameters were determined with good accuracy. Final values of the parameters are given in Table 7, along with the best-fit (CALC) and experimental (EXP) values for the rotational constants. The corresponding structural parameters for $H_2Os(CO)_4$[17] are also listed in Table 7 for comparison with the $H_2Fe(CO)_4$ values. We note that the H−M−H and equatorial C−M−C angles are nearly identical for these complexes. Bond lengths involving the metal atom are about 0.14 Å longer for the osmium hydride complex. The atomic Cartesian coordinates for the "best-fit" structure for $H_2Fe(CO)_4$ are given in Table 8.

Kraitchman Analysis

Spectra were obtained for isotopic substitution of all atoms except oxygen in this complex; therefore, substitution coordinates for each of these substituted atoms could be calculated using the Kraitchman equations for an asymmetric top. Underlying the Kraitchman equations is the assumption that bond lengths and angles do not change upon isotopic substitution. The level of accuracy of this assumption will be discussed and analyzed in the next section. Using this assumption, atomic coordinates (listed in Table 9) for the atoms Fe, H, $C1_{eq}$, and $C3_{ax}$ are obtained that are in good agreement with the parameters determined in the least-squares fit (see Tables 7 and 8). The only constraints on the geometry resulted from the requirement of C_{2v} symmetry for the molecule, and this assumption is supported by both the theoretical calculations (discussed below) and the experimental results. The substitution coordinates are listed in Table 9, and the bond lengths and angles determined from these coordinates are listed in Table 10. The quadratic nature of the principal moments of inertia results in nonzero root-mean-square (rms) coordinates for substituted atoms. The coordinates which are nonzero due to these vibrational effects are marked by a superscript *a* in Table 9. The normal average values for these coordinates are assumed to be zero when

Table 6. Best-fit Spectral Parameters for $^{56}FeHD(CO)_4$, $^{56}FeD_2(CO)_4$, $^{13}C1$(axial), and $^{13}C3$(equatorial) Isotopomers[a]

parameter	units	$^{56}FeHD(CO)_4$	$^{56}FeD_2(CO)_4$	$^{13}C1$(ax)	$^{13}C3$(eq)
A	MHz	1341.3036(6)	1329.7292(9)	1351.3045(6)	1343.4734(4)
B	MHz	1032.6008(6)	1028.4788(10)	1029.1206(7)	1035.0628(5)
C	MHz	924.9188(14)	923.230(3)	921.5845(21)	923.4483(11)
D_J	kHz	0.15(1)	fixed	fixed	0.15(2)
D_{JK}	kHz	fixed	fixed	0.43(2)	0.37(3)
D_K	kHz	−0.22(9)	−0.28(5)	fixed	fixed
δ_J	Hz	−26(11)	fixed	fixed	fixed
δ_K	kHz	0.94(10)	1.1(3)	fixed	fixed
σ_{fit}	kHz	1.3	1.7	1.1	0.6

[a] The listed uncertainties are 2σ.

Table 7. Results of the Least-Squares Fit to Determine Structural Parameters for Tetracarbonyldihydroiron from Experimental Rotational Constants[a]

	A		*B*		*C*	
isotopomer	EXP	CALC	EXP	CALC	EXP	CALC
normal	1353.137	1353.067	1036.633	1036.749	926.742	926.881
^{54}Fe	1353.791	1353.721	1037.015	1037.133	926.725	926.881
^{57}Fe	1352.816	1352.745	1036.445	1036.560	926.751	926.881
HD	1341.304	1341.382	1032.601	1032.488	924.919	924.775
DD	1329.729	1329.931	1028.479	1028.131	923.230	922.800
$^{13}C1$	1351.304	1351.308	1029.121	1029.115	921.585	921.591
$^{13}C3$	1343.473	1343.407	1035.063	1035.174	923.448	923.588

Bond Lengths (Å)			
Fe−H1	1.576(64)	Os−H1	1.720(11)
H1−H2	2.189	H1−H2	2.40(2)
Fe−C1	1.815(54)	Os−C1	1.958(12)
Fe−C3	1.818(65)	Os−C3	1.968(16)
C1−O1	1.123(80)	C1−O1	1.13
C3−O3	1.141(74)	C3−O3	1.13
Interbond Angles (deg)			
H1−Fe−H2	88.0(2.8)	H1−Os−H2	88.3(7)
C1−Fe−C2	154.2(4.2)	C1−Os−C2	163(3)
C3−Fe−C4	99.4(4.3)	C3−Fe−C4	99(2)
Fe−C1−O1	172.5(5.6)	Os−C1−O1	174(5)
Fe−C3−O3	177.8(6.8)	Os−C3−O3	178(4)

[a] Frequencies are in MHz, and the standard deviation for the fit is 0.22 MHz. EXP are the rotational constants obtained from fitting the measured lines, and CALC are the values calculated in the least-squares fit. Indicated errors on the parameters are 2σ. In the second section, right half, the bond lengths and angles for $H_2Os(CO)_4$[17] are shown for comparison.

Table 8. Cartesian Atomic Coordinates (Å) in the Principal Axis System for Tetracarbonyldihydroiron[a]

atom	*a*	*b*	*c*
C1	1.769	0.000	0.705
C2	−1.769	0.000	0.705
O1	2.821	0.000	1.097
O2	−2.821	0.000	1.097
C3	0.000	1.387	−0.877
C4	0.000	−1.387	−0.877
O3	0.000	2.285	−1.580
O4	0.000	−2.285	−1.580
H1	0.000	−1.094	1.433
H2	0.000	1.094	1.433
Fe1	0.000	0.000	0.299

[a] These coordinates were obtained from the least-squares fit to the measured rotational constants, and uncertainties are approximately 0.03 Å.

calculating the internal coordinates listed in Table 10. Forcing the values marked *a* in Table 9 to zero during the calculation of internal coordinates is equivalent to setting the appropriate ΔP_{ii} values to zero. The large zero-point deviations that are often listed as nonzero ΔP_{ii} values (such as the inertial defect in quasi-planar molecules) are then represented by the nonzero coordinate values (marked *a*) in Table 9. The zero-point

Table 9. Substitution (*a*,*b*,*c*) Coordinates in the Center of Mass Frame, Obtained Using Kraitchman's Equations

substituted atom(s)	*r* (Å)	*a* (Å)	*b* (Å)	*c* (Å)
^{54}Fe	0.303	0.048[a]	0.052[a]	+0.294[b]
^{57}Fe	0.303	0.052[a]	0.052[a]	+0.294
D	1.771	0.393[a]	±1.091	+1.452
D_2	1.774	0.390[a]	±1.058	+1.481
$^{13}C1_{ax}$	1.889	±1.747	0.017[a]	+0.719
$^{13}C3_{eq}$	1.640	0.030[a]	±1.388	−0.876

[a] For a C_{2v} symmetry molecule, these average values should be zero; however, Kraitchman analysis gives rms coordinates which are nonzero due to vibrational averaging. [b] Signs indicate on which side of the COM the atoms are found; ± indicates that equivalent atoms are found on either side of the indicated axis.

Table 10. Internal Coordinates for the Substitution Geometry Determined Using the Kraitchman Equations[a]

parameter	value (Å)	parameter	value (deg)
r_s(Fe−H)	1.590(4)	∠H−Fe−H	86.7
r_s(Fe−C1)	1.798(17)	∠C1−Fe−C2	152.7
r_s(Fe−C3)	1.815(30)	∠C3−Fe−C4	99.7

[a] For accurate equilibrium distances, it was necessary to assume the values marked *a* in Table 9 are averaged to zero in the equilibrium geometry.

vibrational motion is quite small for the heavy Fe atom and C atoms but becomes much larger for the low-mass H atoms. As mentioned in the data analysis section, the presence of vibrational averaging can also be observed in the small deviations between the *C* rotational constants for the different Fe isotopomers.

Analysis of H and D Bonding

For most of the atoms in "rigid" molecules, the assumption that the bond lengths and angles in a molecule do not change during isotopic substitution is reasonably accurate and useful. However, when the atoms involved in the bonding are hydrogen and the potential energy function is quite anharmonic, then the large change in zero-point energy due to isotopic substitution can significantly alter the vibrationally averaged (r_0) bond distance. This effect is largest in molecules where deuterium is substituted for hydrogen. There is much data on this "bond shortening" on deuterium substitution for molecules in the first three rows of the periodic table, and bond shortening observed is typically a few thousandths of an angstrom. This effect is much larger in transition metal hydrides, and only a few examples have been studied.[10,11,17] Therefore, it is useful to examine these effects for $FeH_2(CO)_4$.

It was noted from the least-squares fit results that the largest deviations for rotational constants were for the $FeD_2(CO)_4$ data. This was a good indication that the r_0 coordinates for hydrogen were changing on deuterium substitution, since most of the data included in the fit involved only hydrogen atoms. This type of

Table 11. Bond Lengths and Interbond Angles Obtained from Analyses of H and D Bonding[a]

	EXP		DFT	
parameter	X = H	X = D	X = H	X = D
r_{Fe}(X−X) (Å)	2.195	2.131	2.04	2.03
r(Fe−X) (Å)	1.596	1.545	1.55	1.54
∠X−Fe−X (deg)	88.4	87.1		
r_{Os}(X−X) (Å)	2.412	2.379	2.15	2.14
r(Os−X) (Å)	1.728	1.711	1.68	1.67
∠X−Os−X (deg)	88.47	88.10		

[a] Parameters for the Fe−H and Fe−D bonding are shown in the first three rows . The EXP columns EXP are parameters independently determined using the least-squares fit as described in the third section of data analyses. The DFT columns DFT are results of perturbation theory applied to find the average position of the H (D) atoms in the DFT-calculated potential well of the Fe−H symmetric stretch. The last three rows give similar parameters for $H_2Os(CO)_4$ (ref 17) for comparison with the $H_2Fe(CO)_4$ values.

effect was observed previously for $HRe(CO)_5$[11] and $H_2Os(CO)_4$.[17] We believe that the coordinates of all atoms other than hydrogen are much less subject to vibrational averaging effects than the hydrogen atom coordinates for our least-squares fits. Therefore, the moments of inertia of the $Fe(CO)_4$ fragment were calculated using the "best-fit" atomic coordinates shown in Table 8. It is important to calculate these moments in the center of mass (COM) system for $FeH_2(CO)_4$ to obtain the H atom coordinates, and separately, in the COM system for $FeD_2(CO)_4$ to obtain the D atom coordinates. The appropriate $Fe(CO)_4$ "fragment" moments could then be subtracted from the experimental moments of inertia to obtain the contributions to the moments due to only the H or D atoms. The resulting "H fragment", or "D fragment" moments ($\Delta I_{cc} = I_{cc} - I_{cc}'$, etc.) are completely described by the H, D masses and coordinates in the respective COM systems. The equations for these moments and coordinates are as follows:

$$\Delta I_{cc} = 2m_{H,D}b^2, \quad \Delta I_{bb} = 2m_{H,D}c^2, \quad \Delta I_{aa} = 2m_{H,D}r^2 \quad (3)$$

$$b = (\Delta I_{cc}/2m_{H,D})^{1/2}, \quad c = (\Delta I_{bb}/2m_{H,D})^{1/2},$$
$$r = (\Delta I_{aa}/2m_{H,D})^{1/2} \quad (4)$$

An equivalent analysis was performed in which the moments of each fragment were calculated in the center of mass frame for that fragment, and the effects of the shifts of the COM's were taken into account. The coordinates obtained from each of the two analyses were identical. The results of these analyses are shown in Table 11. We have also included some parameters for $H_2Os(CO)_4$[17] for comparison. The *b* and *c* coordinates are transformed to the internal coordinate frame (with Fe at the origin) to show how substitution affects the Fe−H bond distance and the H−Fe−H bond angle. As we would expect, the Fe−H bond distance is longer than the Fe−D bond distance, with the r_0 value from the least-squares fit falling between these two values. The bond angle also contracts upon deuteration, but this is a smaller effect, and the contraction is not much larger than the errors associated with the assumptions and fitting errors. This analysis of "fragment" inertial moments does allow for the introduction of further errors but provides a much better indication of the magnitude of isotope effects on bond lengths than simply comparing Kraitchman and least-squares fit results. The most significant problem is due to the lack of ^{18}O data, which renders the oxygen atom coordinates less precise. The accuracy of moments of inertia depends primarily on the accuracy of coordinates for heavy atoms that have large coordinates off the axis in question. Thus, we believe, the accuracy in the Fe atom position will not greatly affect the accuracy of the fragment moments, or total moments, because it lies close to the center of mass, but the oxygen atoms all lie greater than 2.5 Å from the center of mass and thus have several large coordinate values, and the error in these coordinates will strongly contribute to errors in inertial moments. The 0.05(4) Å Fe−H bond length contraction indicates a large anharmonicity contribution in the Fe−H potential function. We have included a generous estimated "propagation of error" contribution to the error in this difference, following the above discussion. Even though this estimated error is significant, it appears that the isotope effect is real and large. Other typical values for bond length contraction upon deuteration are less than 1 pm.[21] This large isotopic effect is similar in magnitude to results obtained for the other transition metal hydrides.[11,12,17]

Table 12. Comparison of r_o (Least-Squares Fit), r_s (Kraitchman), DFT (Density Functional Theory), and Electron Diffraction Structural Parameters

parameter	least-squares	Kraitchman	DFT (6-311G)	electron diffraction[b]
r(Fe−H) (Å)	1.576(64)	1.590(4)	1.525	1.556(21)
r(Fe−C3) (Å)	1.815(54)	1.798(17)	1.791	1.802(3)
r(Fe−C1) (Å)	1.818(65)	1.815(30)	1.782	1.832(3)
r(C3−O3) (Å)	1.123(80)	na[a]	1.177	1.145(3)
r(C1−O1) (Å)	1.141(74)	na	1.175	1.145(3)
∠H−Fe−H (deg)	88.0(2.8)	86.7	82.41	100.0(10.2)
∠C3−Fe−C4 (deg)	99.4(4.3)	99.7	100.72	96.0(0.6)
∠C1−Fe−C2 (deg)	154.2(4.2)	152.7	150.97	148.5(1.5)
∠Fe−C3−O3 (deg)	177.8(6.8)	na	177.43	fixed (180)
∠Fe−C1−O1 (deg)	172.5(5.6)	na	174.10	fixed (180)

[a] na, not applicable. [b] Reference 18.

DFT Calculations

Calculations were carried out on IBM RISK6000 and SGI Origin 2000 computers at the BPW91 level of density functional theory (DFT), i.e., with the gradient corrections of Becke[22] for exchange and of Perdew and Wang[23] for electron correlation. All calculations employed the Gaussian94 package,[24] revision E.2. The 6-311G basis set was employed for all atoms.

The calculated geometry was in remarkably good agreement with experiment. The calculated rotational constants agreed with the measured values to within 2% for the normal isotopomer. The calculated structure represents a minimum on the multidimensional potential energy surface.[25] This was established by carrying out frequency calculations which produced all real positive frequencies. The internal coordinates from this calculated structure are listed in Table 12 for comparison with other results from this work and with results from the electron diffraction study.

The large isotope effect discussed in the latter part of the structural analyses produced an interest in the anharmonicity of the potential energy surface (PES) in the vicinity of the H atoms. Calculations were done in an effort to map out the one-

(21) Laurie, V. W.; Herschbach, D R. *J. Chem. Phys.* **1962,** *37*, 1687 and references therein.

(22) (a) Becke, A. D. *Phys. Rev.* **1988,** *A38*, 3098. (b) Becke, A. D. *ACS Symp. Ser.* **1989,** *394*, 165. (c) *Int. J. Quantum Chem. Symp.* **1989,** No. 23, 599

(23) Perdew, J. P.; Wang, Y. *Phys. Rev.* **1992,** *B45*, 13, 244.

(24) Frisch, M. J.; Trucks, G. W.; Schlegel, H. B.; Gill, P. M. W.; Johnson, B. G.; Robb, M. A.; Cheeseman, J. R.; Keith, T.; Petersson, G. A.; Montgomery, A. J.; Raghavachari, K.; Al-Laham, M. A.; Zakrzewski, V. G.; Ortiz, J. V.; Foresman, J. B.; Peng, C. Y.; Ayala, P. Y.; Chen, W.; Wong, M. W.; Andres, J. L.; Replogle, E. S.; Gomperts, R.; Martin, R. L.; Fox, D. J.; Binkley, J. S.; Defrees, D. J.; Baker, J.; Stewart, J. P.; Head-Gordon, M.; Gonzalez, C.; Pople, J. A. *Gaussian 94*, Revision B.3; Gaussian, Inc.: Pittsburgh, PA, 1995.

(25) Anet, F. A. L. *J. Am. Chem. Soc.* **1990**, *112*, 7172.

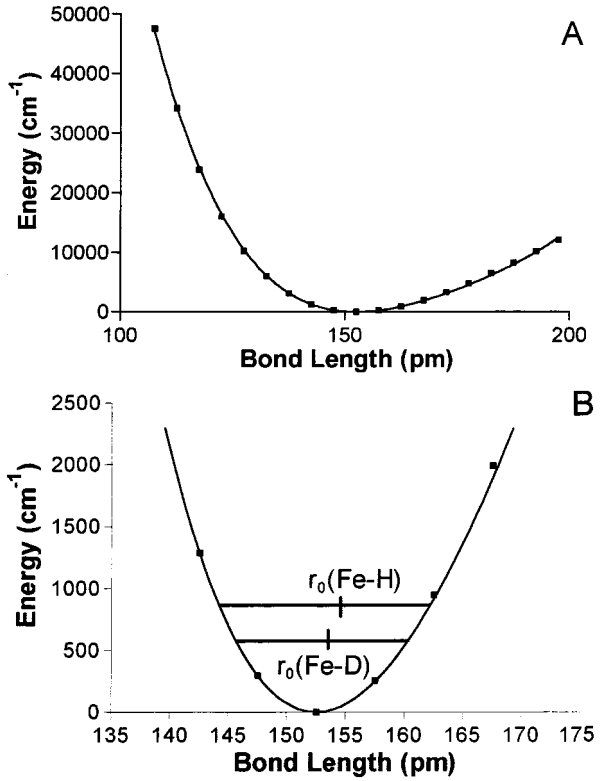

Figure 2. Iron−hydrogen symmetric stretching potential (PES). (A) The full potential energy surface (PES) plot. The smooth curve represents the function E (cm^{-1}) = $10.82(2)\Delta r^2 - 0.190(1)\Delta r^3 + 0.0019(1)\Delta r^4$ ($\Delta r = r - 152.54$ pm, $R^2 = 0.9997$). These parameters were determined with a nonlinear fitting routine. (B) An expanded view of the bottom of the PES with the zero-point energies of the Fe−H and Fe−D and the values for r_0 in each of these levels.

dimensional potential energy surfaces for the symmetric Fe−H stretch and symmetric H−Fe−H bend. The bond length was incremented by 0.05 Å (5 pm) and the H−Fe−H angle by 3° for successive calculations. Both surfaces show interesting features, and these are shown in Figures 2 and 3. The Fe−H stretch PES shows a strong anharmonicity contribution, with the nonlinear regression indicating the cubic term only 50 times smaller than the quadratic coefficient. The values for these coefficients were used in a perturbation theory treatment to calculate the (corrected) wave function for $v = 0$ and then to obtain the mean displacement of the bond length (r_0) from the bottom of the well at $r_e = 1.5254$ Å. Since these r_0 values depend strongly on the reduced mass of the system, two different values were obtained for hydrogen and deuterium. The difference between these two values is a theoretical estimate for the second-order isotope effect discussed in the above structural analysis section. For comparison of the calculated (DFT) and measured isotope effects on the Fe−H (D) bond length, see Table 11. The calculated value for this isotopic shift in r_0 is significantly smaller than the experimental values.

The H−Fe−H symmetric bend PES(see Figure 3) looks very nearly harmonic near the bottom of the well (±15°), indicating that the mean displacement of the atoms from the (calculated) angle 82.4° is very small. This result is supported by the relatively small change in the H−Fe−H angle upon deuteration. The interesting features of this PES occur when the angle becomes small. At an angle of 27°, the H atoms approach to approximately the distance of a molecular hydrogen bond, and there is a local minimum in energy. This angle would correspond to formation of a "dihydrogen" complex, and this is the structure which would be observed if the energy of this

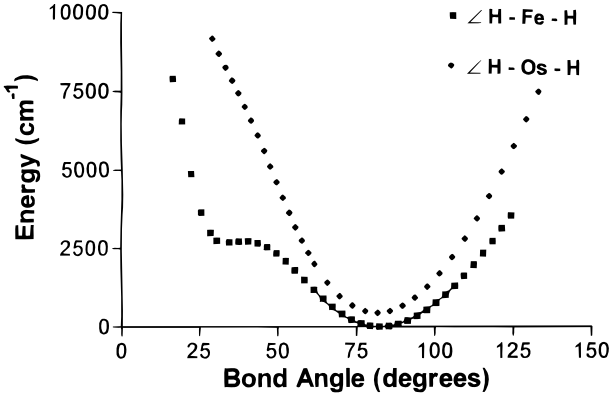

Figure 3. Potential energy surface (PES) for the H−Fe−H bending angle (shown as (■). The bottom part of the well is nearly harmonic. This is represented by the function E (cm^{-1}) = $2.65(4)\theta^2 - 0.0096(7)\theta^3 - 0.0003(1)\theta^4$ ($\theta = \angle$HFeH − 82.38°) This function fits the points between $\theta = 55°$ and 100° (with $R^2 = 0.9992$). The interesting features of this PES occur at small values of ∠HFeH, where H−H interaction causes a local minimum near 28°, as the energy is rapidly rising. This local minimum occurs an H−H distance which would result in a "dihydrogen" type complex. Also plotted (shown as ●) is the PES for ∠HOsH, for the similar $H_2Os(CO)_4$ complex. The PES for ∠HOsH does not show the local minimum near 28°. Energy values are relative to the global minimmum value for $H_2Fe(CO)_4$ and the minimum value −500 cm^{-1} for $H_2Os(CO)_4$.

local minimum were lower than the present global minimum at 80°. As this angle is reduced further, the "H_2" group is pushed away from the Fe atom as the potential energy rises, with the H−H distance remaining rather constant as the Fe−H distance increases. The situation just described suggests a pathway for dissociation through loss of H_2, a known decomposition product. The PES of the H−Fe−H angle is very shallow, the small "dihydrogen" well only about 3000 cm^{-1} above the ground state, indicating a possible reason for the thermal instability of this molecule.

Conclusions

This study provided a reasonably complete experimental and theoretical structural analysis of the transition metal complex tetracarbonyldihydroiron. These results for the structure are in good agreement with previous results of a gas-phase electron diffraction (GED) study.[18] The experimental microwave bond lengths are in very good agreement with the GED bond lengths (see Table 12). The bond angles are more accurately determined in the present microwave study but still agree with the GED data to within quoted error limits. The substitution structure is very close to the DFT structure for iron−carbon parameters and deviates only slightly for the iron−hydrogen parameters. The DFT calculations provide helpful insight on the subtle changes in molecular structure upon isotopic substitution and surprisingly accurate values for the calculated structural parameters. The large deuterium isotope effect was apparent in both the experimental and the calculated structures. Since the experimental elongation of the Fe−H(D) bond length is larger than the calculated effect, it is reasonable to assume that the real PES for the symmetric Fe−H stretch is more anharmonic than the calculated PES.

Acknowledgment. We are extremely grateful to the National Science Foundation (Grant CHE-9634130) for support of this research. Robert Thompson, who was supported by the University of Arizona/NASA Space Grant Undergraduate Research Internship Program, provided help with some of the spectra.

JA9741584